

Correlation between product purity and process parameters for the synthesis of $\text{Cu}_2\text{ZnSnS}_4$ nanoparticles using microwave irradiation

R. Ahmad · K. S. Nicholson · Q. Nawaz · W. Peukert · M. Distaso 

Received: 4 March 2017 / Accepted: 15 June 2017 / Published online: 7 July 2017
© Springer Science+Business Media B.V. 2017

Abstract Kesterites ($\text{CZT}(\text{S},\text{Se})_4$) emerged as a favourable photovoltaic material, leading to solar cell efficiencies as high as 12.7%. The development of sustainable roll-to-roll printing processes that make use of $\text{Cu}_2\text{ZnSnS}_4$ (CZTS) nanoparticle inks requires the proper design of synthetic approaches and the understanding of the relation between process parameters and product purity. In the current paper, we developed this relationship by calculating a specific energy factor. A microwave-assisted synthetic method that operates at atmospheric pressure and makes use of eco-friendly solvents is established. Four solvents, i.e. ethylene glycol (EG), diethylene glycol (di-EG), triethylene glycol (tri-EG) and tetraethylene glycol (tet-EG) are compared and the temperature during the reaction is assessed by two different methods. In particular, two by-products have been identified, i.e. Cu_{2-x}S and a hexagonal phase. We show that the variation of reaction parameters such as power irradiation, type of solvent and precursor concentration

influences the nanoparticles' sizes (from 12 to 6 nm) and also the temperature-time profile of reaction which, in turn, can be related to phase purity of CZTS nanoparticles. The results suggest that the product purity scales with the specific energy factor providing a useful tool to a rational design of high-quality CZTS nanoparticles.

Keywords Solar cells · Kesterite · Disordered CZTS · Cubic CZTS · Green chemistry · Photovoltaics · Energy conversion

Introduction

From household use to spacecraft, photovoltaic has been proving to be a reliable technology for energy production. The implementation of solar cells that make use of non-toxic and cost-effective materials and processes paves the way for a sustainable solution to the current and future energy problems. Kesterites ($\text{CZT}(\text{S},\text{Se})_4$) emerged as a favourable photovoltaic material, leading to solar cell efficiencies as high as 12.7% (Kim et al. 2014). $\text{Cu}_2\text{ZnSnS}_4$ (CZTS) consists of earth-abundant and benign elements, and with its band gap of 1.45 eV, a practical conversion efficiency higher than 20% is expected (Siebentritt 2013). Thin films have been produced by various vacuum deposition techniques such as sputtering, pulsed layer deposition and chemical vapour deposition (Hermes et al. 2015). However, processes for the production of CZTS layers that avoid the use of vacuum as well as of high pressure are required for a sustainable industrial roll-to-roll process.

Electronic supplementary material The online version of this article (doi:10.1007/s11051-017-3932-5) contains supplementary material, which is available to authorized users.

R. Ahmad · K. S. Nicholson · Q. Nawaz · W. Peukert · M. Distaso (✉)
Institute of Particle Technology, Friedrich-Alexander-Universität Erlangen-Nürnberg, Cauerstraße 4, 91058 Erlangen, Germany
e-mail: monica.distaso@fau.de

R. Ahmad · K. S. Nicholson · Q. Nawaz · W. Peukert · M. Distaso
Interdisciplinary Center for Functional Particle Systems, FAU Erlangen-Nuremberg, Haberstraße, 9a, 91058 Erlangen, Germany

CZTS nanoparticles offer a viable route towards continuous printing processes through the formulation of suitable inks (Choi et al. 2015). This technology would enable a sustainable layer production on flexible substrates (Choi et al. 2015); however, it requires the development of robust methods for the wet production of CZTS nanoparticles. The state of the art in the literature shows that CZTS nanoparticles have been synthesized in liquid phase by a hot-injection method (Ghorpade et al. 2014), under solvothermal and hydrothermal conditions (Zhou et al. 2013), and also by using microwave irradiation (Morschhäuser et al. 2012; Knutson et al. 2014; Zhao et al. 2015a). The hot-injection method requires prolonged heating time at a minimum temperature as high as 225 °C (Ghorpade et al. 2014). The scalability of the hot-injection processes is challenging due to limited control and flexibility with regard to injection at high temperature while maintaining fast and sufficient mixing. Therefore, a non-injection approach is preferable (van Embden et al. 2015). Furthermore, the synthesis is performed in the presence of long-chain surfactants that are adsorbed on the surface of the particles after the synthesis and that have to be eliminated to improve the communication at particle-particle interfaces and, hence, the device performance. Accordingly, additional post-processing steps such as annealing under controlled Sn and/or S atmospheres (Delbos 2012; Choi et al. 2015) or ligand exchange (Carrete et al. 2013) were carried out. Synthesis under solvothermal and hydrothermal conditions implies the use of closed vessels, usually stainless steel autoclaves, where the so-called “autogenous pressure” is established, according to the vapour pressure of the used solvent at the working temperature (Distaso et al. 2012b; Zhou et al. 2013). Also, in this case, heating at high temperatures (>200 °C) for several hours is necessary for batch and semi-batch processes (Cui et al. 2009; Chen et al. 2014; Yan et al. 2015).

The use of microwaves is considered one of the most eco-friendly and efficient heating methods in comparison to conventional approaches as it provides a faster and more homogeneous heating of the reaction mixtures by the interaction of the electric field with the dipoles and ions in solution (Cushing et al. 2004). Therefore, we believe that a microwave-assisted process at atmospheric pressure for the synthesis of CZTS nanoparticles provides a highly efficient route towards the production of this material. Organic chemistry has been extensively studied under microwave conditions. As a result, the synthesis of organic compounds with a throughput of 20 L/h (500 L/day) has been recently demonstrated using a microwave flow system

(Morschhäuser et al. 2012). In comparison, considerably less work has been devoted to inorganic materials, such as Au, Ag, ZnO and CdTe/CdS (Carrete et al. 2013; Chen et al. 2014; Delbos 2012; Yan et al. 2015; Distaso et al. 2012a; Gerbec et al. 2005; He et al. 2006), or tri- and tetra-element systems, such as CuInS₂ (Pein et al. 2011), CuInSe₂ (Wu et al. 2010), CuIn_xGa_{1-x}S₂ (Sun et al. 2010; Bilecka and Niederberger 2010) and Cu₂ZnSnS₄ (Flynn et al. 2012; Knutson et al. 2014). Thermolysis of precursor solutions deposited on substrates leading to CZTS films has also been reported (Knutson et al. 2014; Zhao et al. 2015b).

In particular, the synthesis of multicomponent nanoparticles using microwaves can be of high value, as the purity of products may critically depend on the mixing efficiency and homogeneity of the overall reaction mixture. The better the elemental and temperature homogeneity, the lower is the chance of formation of by-products. Although papers describing the microwave-assisted synthesis of CZTS nanoparticles are readily available in the literature (Bilecka and Niederberger 2010; Shin et al. 2012; Wang et al. 2013; Knutson et al. 2014; Lin et al. 2015; Zhao et al. 2015a), a relation between process parameters and phase homogeneity of CZTS nanoparticles has not been demonstrated so far. Furthermore, most of the published works make use of closed vessels with consequent high pressure during the process (Flynn et al. 2012; Wang et al. 2013) or of multimode¹ microwave heating either by household microwave ovens or laboratory instruments. In these devices, temperature inhomogeneities occur and assessment of the reaction temperature is inaccurate and unreliable. Apart from the work of Flynn et al. (2012), no report provides reliable temperature measurement which is not only of primary importance in any synthetic protocol but is also fundamental for reactions under microwave irradiation in general (Dudley et al. 2015). Recently, Martini et al. (2016) described a method to realize CZTS thin films using nanoparticles derived from a continuous-flow microwave-assisted synthesis. In order to obtain crystalline particles, the low-crystalline as-synthesized material is dried in vacuum at 300 °C and the corresponding thin films were annealed in sulphur-containing atmosphere at 540 °C. We believe that a better understanding of the influence of the chosen solvent, precursor concentration and other process parameters would lead to a higher

¹ In multimode setup, the intensity of microwaves (and hence, the temperature) may vary from one point of the reactor to another, depending upon arbitrary interference of microwaves.

crystalline material and to an improvement of the energetic balance of the entire process chain from molecules to thin films. Therefore, in the current paper, we present a non-solvothermal approach for the synthesis of CZTS nanoparticles without the use of any inert/vacuum atmosphere or high pressure and using a mono/single-mode² microwave heating cavity with a reliable assessment of temperature during the reaction.

We compare four eco-friendly solvents, i.e. ethylene glycol (EG), diethylene glycol (di-EG), triethylene glycol (tri-EG) and tetraethylene glycol (tet-EG) and estimate the temperature during our reaction by two different methods. This leads to a better understanding of the effect of synthesis parameters on the control of temperature-time profile of the reaction and formation of CZTS phase. Based on the temperature-time profile, we propose a specific energy factor that can be used to estimate reaction conditions and predict the CZTS phase purity. To the best of our knowledge, a correlation between reaction conditions in microwave synthesis and CZTS phase purity has never been established before. Lastly, we show that the most widely used solvent EG is not optimal for reactions under atmospheric pressure whereby, a systematic optimization of process parameters leads to a higher-purity product while using tet-EG as a solvent.

Methods

Materials

Copper(II) acetate anhydrous ($\text{Cu}(\text{O}_2\text{CCH}_3)_2$, 98%; Alfa Aesar, Germany), zinc acetate dihydrate ($\text{Zn}(\text{O}_2\text{CCH}_3)_2 \cdot 2\text{H}_2\text{O}$, 99.5%; Merck, Germany), tin(II) acetate ($\text{Sn}(\text{O}_2\text{CCH}_3)_2$; Aldrich, Germany) and thiourea (Merck, Germany) were used as copper, zinc, tin and sulphur sources, respectively. Further, toluene (99.5%; Carl Roth, Germany), distilled water (Milli-Q) and absolute ethanol (99.8%; Alfa Aesar, Germany) were used.

EG ($\geq 99\%$; Carl Roth, Germany), di-EG ($\geq 99\%$; Carl Roth, Germany), tri-EG (99%; Sigma-Aldrich, Germany) and tet-EG (99%; Aldrich, Germany) were chosen

as the solvents. All chemicals were used as received without any further purification.

Synthesis of CZTS nanoparticles

To synthesize CZTS nanoparticles, the metal salt precursors in their stoichiometric ratio were dissolved in 30 mL of the given solvent. Namely, in the standard approach, $\text{Zn}(\text{O}_2\text{CCH}_3)_2 \cdot 2\text{H}_2\text{O}$ (0.5 mmol), $\text{Sn}(\text{O}_2\text{CCH}_3)_2$ (0.5 mmol) and $\text{Cu}(\text{O}_2\text{CCH}_3)_2$ (1 mmol) were dissolved in 30 mL of the given solvent with the help of ultrasonication for 30 min. Afterwards, thiourea (2.5 mmol) was added and the solution was stirred for 2 min at room temperature. This concentration of precursors is marked as “x”. In some experiments, the concentration of each starting salts and that of thiourea were halved, doubled and tripled (Tables 1 and 2), keeping the ratio constant. Each solvent showed a different degree of solubilization of the metal precursors. An overview is presented in Supporting Information (Additional file 1: Table S1). The as-obtained mixtures were then treated with microwaves for 30 min at a given power using the commercially available lab reactor “CEM Discover LabMate”. The instrument was controlled by the software “Synergy”. The device incorporates an infrared temperature sensor at the bottom of the reaction chamber. An additional non-mercury thermometer (Easy Read[®]; Sigma-Aldrich, Germany) filled with a non-hazardous and eco-friendly fluid having an accuracy of ± 3 °C was fixed inside the reflux column to estimate the temperature directly inside the reaction mixture. A video camera was used to record the temperature changes over time from the immersed thermometer. In order to identify the best operating conditions for the microwave reactor, different *methods* available in the software were investigated using distilled water and toluene. The detailed analysis in this regard is provided in Supporting Information (Additional file 1: Figure S1).

Upon completion, the reaction mixture was cooled to 50 °C by a flux of compressed air and then 40 mL of absolute ethanol was added to the reaction mixture and the suspension was centrifuged for 30 min at a relative centrifugal force of ~ 2410 to separate particles from the parent solvent. This step was repeated several times (depending upon solvent) until a clear supernatant was obtained. The precipitates were then air-dried to powder for further characterization. The particles were found to

² In a mono-mode cavity, a more homogenous microwave field (and hence, temperature) is achieved (standing wave), leading to energy efficiency 10 times higher than that in a multi-mode cavity.

Table 1 A summary of EDX analysis and maximum temperature obtained for different CZTS nanoparticle powders synthesized under specified reaction conditions

Solvent	Conc.	T (°C)	Cu/(Zn + Sn)	Zn/Sn	S/Zn	S/Sn	S/Cu
EG	x	192	1.21 ± 0.05	1.70 ± 0.14	3.48 ± 0.31	5.88 ± 0.31	1.81 ± 0.12
Di-EG	x	180	1.07 ± 0.08	1.10 ± 0.09	3.69 ± 0.24	4.07 ± 0.34	1.81 ± 0.10
Tri-EG	x	172	1.22 ± 0.06	1.09 ± 0.16	4.03 ± 0.27	4.37 ± 0.42	1.71 ± 0.06
Tet-EG	x	162	1.27 ± 0.08	1.58 ± 0.16	3.79 ± 0.22	5.97 ± 0.52	1.82 ± 0.06
Tet-EG	x	192	1.25 ± 0.07	1.34 ± 0.15	3.78 ± 0.37	5.00 ± 0.27	1.71 ± 0.07
Tet-EG	x	221	1.02 ± 0.32	1.15 ± 0.10	4.06 ± 0.74	4.63 ± 0.75	2.19 ± 0.31
Tet-EG	$x/2$	201	1.06 ± 0.07	1.03 ± 0.08	4.29 ± 0.23	4.41 ± 0.20	2.05 ± 0.09
Tet-EG	$2x$	237	0.84 ± 0.03	0.88 ± 0.04	4.29 ± 0.20	3.78 ± 0.13	2.40 ± 0.09
Tet-EG	$3x$	247	0.83 ± 0.06	0.86 ± 0.05	4.42 ± 0.33	3.87 ± 0.13	2.51 ± 0.13

$x = \text{Zn}(\text{O}_2\text{CCH}_3)_2 \cdot 2\text{H}_2\text{O}$ (0.5 mmol), $\text{Sn}(\text{O}_2\text{CCH}_3)_2$ (0.5 mmol), $\text{Cu}(\text{O}_2\text{CCH}_3)_2$ (1 mmol) and thiourea (2.5 mmol) in 30 mL of the given solvent. $x/2$, $2x$ and $3x$ represent the halved, doubled and tripled concentrations, respectively (see the experimental part)

be re-dispersible in water and in polar organic solvents such as ethanol upon ultrasonication.

X-ray diffraction (XRD) analysis was performed using a D8 Advance instrument (Bruker AXS GmbH, Germany) with Cu K_α radiation ($\lambda = 1.5406 \text{ \AA}$). The sample holders comprise of low-background sample cups with a vicinal (911) Si crystal of 25 mm diameter (Bruker AXS GmbH). The samples were prepared by spreading a layer of dried powder on the Si crystal. All the presented patterns were background subtracted.

Raman spectroscopy was performed using confocal micro-Raman (LabRAM HR Evolution; HORIBA),

with LabSpec 6 software, equipped with green (532.1 nm, Nd-YAG) and red (632.8 nm, He-Ne) lasers with an average power on sample surface less than 0.3 and 0.2 mW, respectively. To avoid phase changes due to high-power laser or prolonged laser exposure widely reported in the literature (Fernandes et al. 2011; Ahmad et al. 2013; Dimitrievska et al. 2014), the acquisition parameters were carefully optimized in order to avoid overheating of the sample while maintaining a good spectral quality. The lasers were focused on powdered samples (pressed into a pellet) using a $50 \times$ objective with a nominal spot size of $\sim 1.0 \mu\text{m}$. All presented

Table 2 Summary of energy calculated from the temperature-time profile of the reactions and corresponding specific energy factors

Line	Solvent	Microwave power (W)	Precursor conc.	Calculated total energy, Q_{rxn} (kJ)	Specific energy factor (F) ($Q_{\text{rxn}}/\Delta G_f$ (CZTS))	$\text{Cu}_2 - x\text{S}$ phase (I_{472} / I_{333} (Raman))	Hexagonal phase ($I_{26.85} / I_{28.45}$ (XRD))
1	EG	100	x	7.95	-124.64	^a (Fig. 1c)	0.11 (Fig. 1b)
2	Di-EG	100	x	6.92	-106.23	0.10 (Fig. 1c)	0.14 (Fig. 3d)
3	Tri-EG	100	x	6.17	-93.74	0.30 (Fig. 1c)	0.27 (Fig. 1b)
4	Tet-EG	100	x	5.76	-86.26	0.37 (Fig. 3c)	0.21 (Fig. 3b)
5	Tet-EG	150	x	7.22	-113.78	0.13 (Fig. 3c)	0.14 (Fig. 3b)
6	Tet-EG	200	x	8.45	-139.16	^a (Fig. 4c)	0.10 (Fig. 3b)
7	Tet-EG	200	$x/2$	7.59	-242.45	^a (Fig. 4c)	^a (Fig. 4b)
8	Tet-EG	200	$2x$	8.99	-75.53	^a (Fig. 4c)	0.22 (Fig. 4b)
9	Tet-EG	200	$3x$	9.16	-51.64	^a (Fig. 4c)	0.48 (Fig. 4b)

$x = \text{Zn}(\text{O}_2\text{CCH}_3)_2 \cdot 2\text{H}_2\text{O}$ (0.5 mmol), $\text{Sn}(\text{O}_2\text{CCH}_3)_2$ (0.5 mmol), $\text{Cu}(\text{O}_2\text{CCH}_3)_2$ (1 mmol) and thiourea (2.5 mmol) in 30 mL of the given solvent. $x/2$, $2x$ and $3x$ represent the halved, doubled and tripled concentrations, respectively (see experimental part)

^aNo evidences under the conditions used in this work

spectra were twice accumulated using 120 s as acquisition time and were smoothed and background subtracted.

Energy-dispersive X-ray (EDX) was performed using EDX-ULTRA™ 55 (Carl Zeiss AG, Germany) under an accelerating voltage of 20 kV. The samples were prepared by pressing the powder into a pellet using a handheld press. Each sample was tested at a minimum of 10 different points in the pellet.

Inductively coupled plasma optical emission spectrometry (ICP-OES) was performed using the ICP-OES spectrometer Optima 8300 from PerkinElmer. The samples were prepared by choosing an appropriate dilution of the mother liquor in Milli-Q water.

Scanning electron microscopy (SEM) was performed using ULTRA™ 55 (Carl Zeiss AG, Germany) using a 20 kV acceleration voltage and an InLens detector. The samples were prepared by pressing some powder sample on standard conductive sticky carbon pads.

High-resolution transmission electron microscopy (HRTEM) was performed using a Philips CM 300 UltraTWIN with a nominal point resolution of 0.17 nm at Scherzer defocus. The microscope was operated at 300 kV using a thermionic LaB6 filament. For TEM analysis, the particles were drop casted on standard copper grids, supported with a continuous amorphous carbon film. The image analysis was carried out by using the freeware ImageJ package (Abramoff et al. 2004).

Results

Choice of solvents and their interaction with microwaves

Irrespective of synthesis approaches, so far, only five solvents have been reported for the synthesis of CZTS nanoparticles under microwave irradiation: oleylamine (Wang et al. 2013; Knutson et al. 2014), EG (Flynn et al. 2012; Zhao et al. 2015b), ethylenediamine (Lin et al. 2015), *N,N*-dimethylformamide (Saravana Kumar et al. 2014) and water (Shin et al. 2012), with EG being the most favoured solvent due to its high dielectric constant and low toxicity. In general, the most successful syntheses of CZTS nanoparticles are reported at temperatures equal to or higher than 200 °C (Zhou et al. 2013; Azimi et al. 2014; Kim et al. 2014; Ahmad et al. 2015). Thus, as the aim of this work was to realize a process at atmospheric pressure, solvents with boiling points as

high as 200 °C were selected, ruling out the possibility to use water, *N,N*-dimethylformamide and ethylenediamine as the possible solvent. Other parameters taken into account were the toxicity, costs and, most importantly, the values of the $\tan(\delta)$, the so-called “loss factor” ($\tan(\delta) = \varepsilon'' / \varepsilon'$, where ε'' is the dielectric loss and ε' is the dielectric constant of the solvent). This parameter measures the ability of a substance to absorb microwaves and convert them into heat and can be estimated, in a first approximation, by evaluating the dielectric constant of a given substance. Therefore, oleylamine is also not a favourable solvent because of its low dielectric constant. On these bases, the glycol family of solvents suited the best, and their properties are summarized in Additional file 1: Table S2. In this regard, ethyl glycol represents a borderline case and was also used in our experiments. This also helps to compare our work with the state of the art.

Microwaves are expected to have *thermal* and *non-thermal* effects on reaction mixtures, the former depending on the actual temperature and the latter implying an interaction of microwaves (MW) with reaction intermediates (Dudley et al. 2015). Up to now, most researchers agreed on the fact that all the advantages of microwaves (such as short reaction times, higher yields and selectivity) are the results of *thermal effects*, where the exact estimation of the temperature inside the reaction mixture is the most important and controversial factor (Bilecka and Niederberger 2010; Kharissova et al. 2011; Dudley et al. 2015). In our work, a careful measurement of the temperature during the reaction by two different methods was carried out. The relevant details are provided in Supporting Information. The assessment of temperature from the infrared sensor was found unreliable (Additional file 1: Figures S1 and S2) in comparison to the results obtained by the thermometer, with absolute differences larger than 70 °C in some cases (Additional file 1: Table S2). Therefore, only temperature vs. time profiles measured by the glass thermometer are shown in the following.

Influence of solvents with different dielectric constants on the phase purity of CZTS nanoparticles

Figure 1a shows the temperature profiles recorded during the synthesis of CZTS nanoparticles in the corresponding solvents upon irradiation of the reaction mixture with a fixed power of 100 W. The solvent with the highest dielectric constant, i.e. EG,

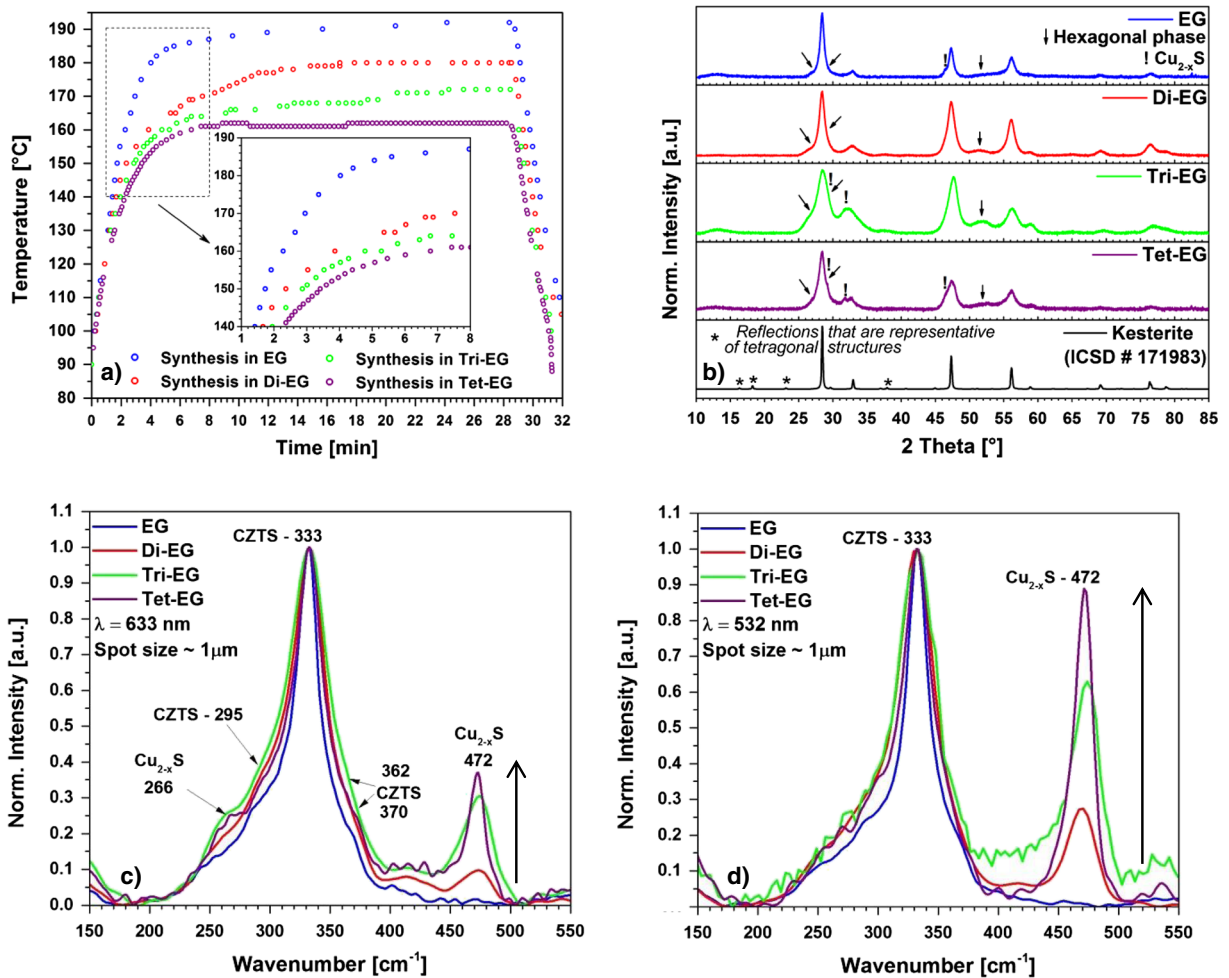


Fig. 1 a Temperature profiles obtained during the synthesis of CZTS nanoparticles in EG, di-EG, tri-EG and tet-EG under a 100 W microwave power. b XRD patterns of the as-synthesized

particles and comparison with the reference CZTS pattern. c, d Raman spectra using *green* and *red* lasers, respectively

reached a higher temperature (192 °C) and was heated faster with respect to the solvent with the lowest dielectric constant, i.e. tet-EG (Additional file 1: Table S2 and Fig. 1a). A comparison of the heating rate and maximum temperature reached during the synthesis with the corresponding curves obtained by heating the pure solvent shows that the former are always faster and at a higher temperature (cf. Additional file 1: Figure S2 and Fig. 1a). The precursors in the reaction mixture are, in fact, also able to absorb microwaves, leading to an additional ionic heating. Moreover, the enthalpies of formation of all possible binary, ternary and quaternary products are negative (Ahmad et al. 2013); i.e. exothermic processes are expected during the course of reaction which must have further contributed to the higher temperature.

The characterization of the resulting particles shows, in fact, that their degree of purity varies considerably with respect to the used solvent. The XRD patterns (Fig. 1b) when taken together with Raman analysis (Fig. 1c, d) confirm the presence of CZTS and Cu_{2-x}S phases, with some reflections from an additional hexagonal phase (marked with arrows). In agreement with the literature and with our previous results, these reflections might be attributed to Cu₃SnS₄ and wurtzite CZTS/Cu_{2-x}S/ZnS or to hexagonal stacking faults in cubic CZTS and are detrimental to the product properties (Flynn et al. 2012; Ahmad et al. 2015). The Raman analysis shows no peak in the region 318 to 320 cm⁻¹; therefore, the possibility that the hexagonal phase is Cu₃SnS₄, wurtzite CZTS and hexagonal stacking faults in cubic CZTS (Ahmad et al. 2013, 2015) can be ruled

out. Therefore, the hexagonal reflections observed in the XRD pattern might be attributed to wurtzite ZnS or to a Raman-inactive Cu_{2-x}S hexagonal phase (Ahmad et al. 2015). These possible secondary phases are indicated with the generic term “hexagonal phase” throughout the paper, being an exact assignment not straightforward (Dimitrievska et al. 2014; Just et al. 2011; Vaccarello et al. 2015).

The EDX analysis on the powder samples shows in all cases the formation of Zn-rich and Sn-poor product (Table 1, Additional file 1: Figure S3). The mother liquor obtained after synthesis in EG was analysed by ICP-OES, and it was found that only 67.6% of Sn was consumed during the reaction in comparison to Zn and Cu, whose conversions were 98 and 99%, respectively.

It must be noted that kesterite in tetragonal structure presents reflections at lower 2θ degrees, i.e. at about 16° , 18° , 23° and 38° (marked with asterisks), that are not observed in our XRD patterns, suggesting the formation of cubic CZTS. Such patterns of cubic CZTS are extensively reported and discussed elsewhere (Ahmad et al. 2013, 2015; Brandl et al. 2015). The Raman spectra (Fig. 1c, d) show a dominant peak at about 333 cm^{-1} which further confirms the formation of CZTS phase in all the solvents (Ahmad et al. 2013). Additionally, the characteristic peak of Cu_{2-x}S is observed at 472 cm^{-1} whose intensity increases, going from EG to tet-EG. For the particles synthesized in tri-EG and tet-EG, a shoulder at

266 cm^{-1} is further observed, ascertaining the presence of Cu_{2-x}S in one of its polymorphs (Ahmad et al. 2015).

The SEM analysis carried out on the powder sample (Additional file 1: Figure S6 in Supporting Information) shows that the particles have irregular morphology. To estimate the average particle sizes, XRD peaks were fitted using the Lorentzian function and FWHM of the three most intense peaks ($\sim 28.46^\circ$, $\sim 47.37^\circ$ and $\sim 56.14^\circ$ (2θ)) was used in the Debye-Scherrer equation. Average particle sizes thus obtained were 12, 8, 6 and 8 nm for product synthesized in EG, di-EG, tri-EG and tet-EG, respectively. To further characterize the morphology, size and crystallinity of the as-synthesized particles, HRTEM was performed on the sample synthesized in EG that showed the highest purity.

An overview of the particles is reported in Fig. 2a, b, where the boundaries of few particles are marked with a white line to facilitate their identification. The HRTEM analysis in Fig. 2c shows that the particles are highly crystalline. A fast Fourier transform (FFT) analysis (Fig. 2d) of full image shown in Fig. 2c shows the presence of different lattice planes. An in-depth analysis results into identification of planar spacings of 1.5, 1.6, 1.9, 2.7, 3.1 and 3.3 \AA , which are based on the FCC unit cell derived from XRD analysis (Fig. 1b), are related to (222), (311), (220), (200) and (111) planes, respectively. Concerning the spacing of 3.3 \AA , it may correspond to the (011) plane in the hexagonal unit cell and, therefore, can be

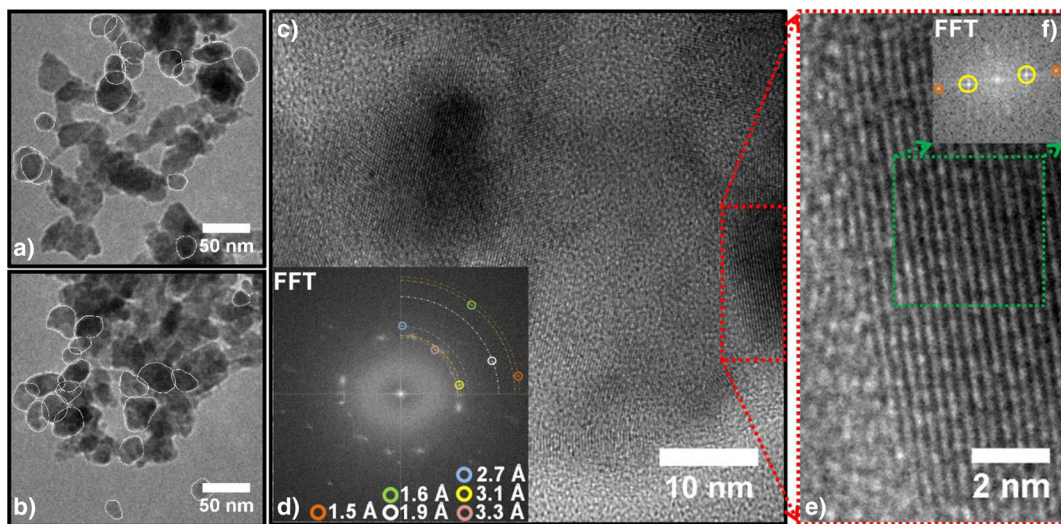


Fig. 2 High-resolution transmission electron micrographs showing **a**, **b** arbitrarily shaped particles synthesized in EG; boundaries of some particles are marked to facilitate their identification; **c** a set of lattice planes from various particles and **d** the fast Fourier

transformation (FFT) of the image in **c** that shows a set of lattice planes spaced at 1.5, 1.6, 1.9, 2.7, 3.1 and 3.3 \AA . **e** A magnified view of one set of planes from the image in **c**. **f** Its FFT (as an example)

attributed to the hexagonal (secondary) phase observed in XRD analysis as well. Additionally, the FFT analysis of the region marked with red in Fig. 2c shows that interplanar spacings of 1.5 and 3.1 Å observed in Fig. 2d are due to (222) and (111) sets of planes, respectively.

In addition to the analysis shown in Fig. 2e, the FFT of another area in Fig. 2c is presented in the supporting information (Additional file 1: Figure S10) as an example for the origin of reflections from the hexagonal phase.

Influence of microwave irradiation power on the phase purity of particles produced in tet-EG

It is evident from the results shown so far that under the given synthesis conditions, EG yielded CZTS with much higher purity with respect to the other solvents, whereby tet-EG resulted in the highest amount of by-products. In particular, Cu_{2-x}S phase and a hexagonal phase could be identified. As one of the aims of the present work was to define the potential of microwave technology towards the control of phase composition of multicomponent materials, a process parameter study was carried out with the aim of improving the final particle purity. As the boiling point of EG is 197 °C, this solvent is not suitable to further increase the process temperature above 192 °C (i.e. already achieved in the first set of experiments (Fig. 1)) under atmospheric conditions. Therefore, tet-EG was used as a test solvent as it has a higher boiling point (329 °C) and therefore offers the highest flexibility to establish a relation between process parameters and product property (phase homogeneity). The CZTS particles obtained when EG was used as a solvent were used as a benchmark (having the least of hexagonal and Cu_{2-x}S phases, Fig. 1). In particular, for a direct comparison of the product purity synthesized in tet-EG, the power of the MW irradiation was varied in order to match the temperature obtained when the used solvent was EG (Fig. 1a).

Figure 3a shows the temperature profiles obtained during the synthesis of CZTS nanoparticles using tet-EG as the solvent under different powers of MW irradiation. As expected, by increasing the irradiation power the maximum temperature achieved in the reaction mixture was also increased. In particular, it was found that with an irradiation power of 200 W, a fast increase of the temperature up to 220 °C, followed by a slight decrease over time, occurred. The slight reduction of the temperature over time can be attributed to the formation of solid particles with various phase compositions, their

different abilities to interact with MW and the degree of their dissolution in different solvents as based on our previous experience, these factors certainly affect the overall temperature of the reaction mixture (Wang et al. 2013; Distaso et al. 2014).

The phase analysis of the as-synthesized nanoparticles is shown in Fig. 3b–d. Taken together, XRD and Raman analyses show that by increasing the power and, consequently, the temperature of the reaction mixture, the amount of Cu_{2-x}S and hexagonal phase decreases. The EDX analysis (Table 1, Additional file 1: Figure S4) also shows that Sn is progressively incorporated in the final product by increasing the irradiation power, leading to the formation of CZTS particles with an elemental composition closer to the ideal stoichiometry of CZTS phase. However, at all temperatures, the formation of only cubic CZTS phase is observed, as the reflections at low 2θ degrees are not visible in any XRD patterns. Further, SEM images show the formation of irregularly shaped particles (Supporting Information - Additional file 1: Figures S7 and S8). The average particle sizes show a slight increase with increasing microwave irradiation power, i.e. 8, 8.8 and 9 nm for 100, 150 and 200 W, respectively.

At this point, it is possible to compare the quality of the CZTS nanoparticles synthesized in tet-EG (at 150 W) and in EG (at 100 W) as the temperature reached for these two solvents is comparable, i.e. ~192 °C. The comparison between the XRD patterns and Raman spectra for these two samples shows that the synthesis in tet-EG has resulted in the formation of more by-products (Fig. 1 vs. Fig. 3). These results indicate that the temperature is not the only factor that influences the selective formation of CZTS, and suggest that the chemical nature of the solvent and its interaction with precursors might also play an important role. Finally, to study the effect of concentration of the precursors on the final product, the following set of experiments was planned with a variable concentration of precursors in tet-EG.

Influence of precursor concentration on the phase purity of particles produced in tet-EG

The different amounts of precursor chosen for these sets of experiments are listed in Table 1; i.e. the amounts were halved, doubled and tripled with respect to the standard *x concentration* corresponding to 0.017 M for the Zn and Sn precursors, 0.033 M for the Cu salt and 0.083 M for thiourea (experimental part). The

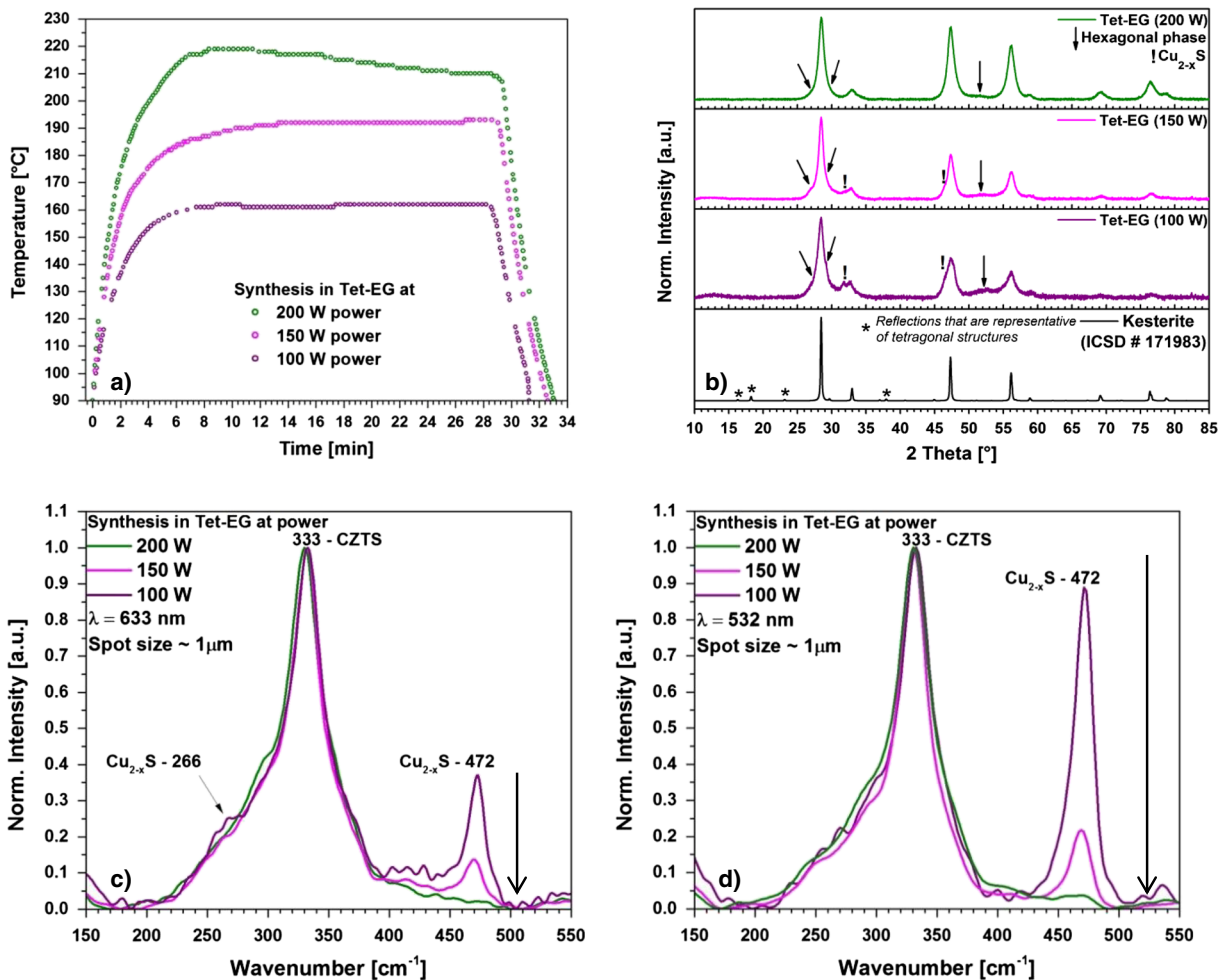


Fig. 3 a Temperature profiles obtained from a thermometer during the synthesis of CZTS nanoparticles in tet-EG under different microwave irradiation powers. b XRD pattern confirming the presence of cubic CZTS, hexagonal phase (impurity) and Cu_{2-x}S .

c, d Raman spectra using red and green lasers, respectively, showing a decreasing amount of Cu_{2-x}S with an increasing temperature or microwave power

corresponding temperature profiles (Fig. 4a) show that the higher the precursor concentration, the stronger the microwave interaction with the reaction mixture and the higher is the temperature. As the reaction proceeds, the overall temperature drops in each case until about 18 min. This is known to be an indication of conversion of ions/precursors into products (Bilecka and Niederberger 2010).

The characterization of the as-synthesized particles reveals irregularly shaped particles as ascertained by SEM analysis (Additional file 1: Figure S8). Raman and XRD analyses show no detectable amounts of Cu_{2-x}S (Fig. 4b–d). However, from the XRD patterns, it is evident that the amount of the hexagonal phase is higher in the product synthesized with a higher

concentration (Fig. 4b, Table 1). The average particle sizes appear to be similar for x and $x/2$ concentrations, i.e. 9 nm, but decrease to 7 and 6.6 nm for $2x$ and $3x$ concentrations, respectively. Accordingly, the EDX analysis shows that the products synthesized at higher concentration are further away from the composition of ideal CZTS. The composition of the products synthesized with x concentration (corresponding to 0.017 M for the Zn and Sn precursors, 0.033 M for the Cu salt and 0.083 M for thiourea, experimental part) or $x/2$ concentration (corresponding to 0.0085 M for the Zn and Sn precursors, 0.0165 M for the Cu salt and 0.0415 M for thiourea, experimental part) is very close to ideal CZTS with no evidence of hexagonal and Cu_{2-x}S impurities.

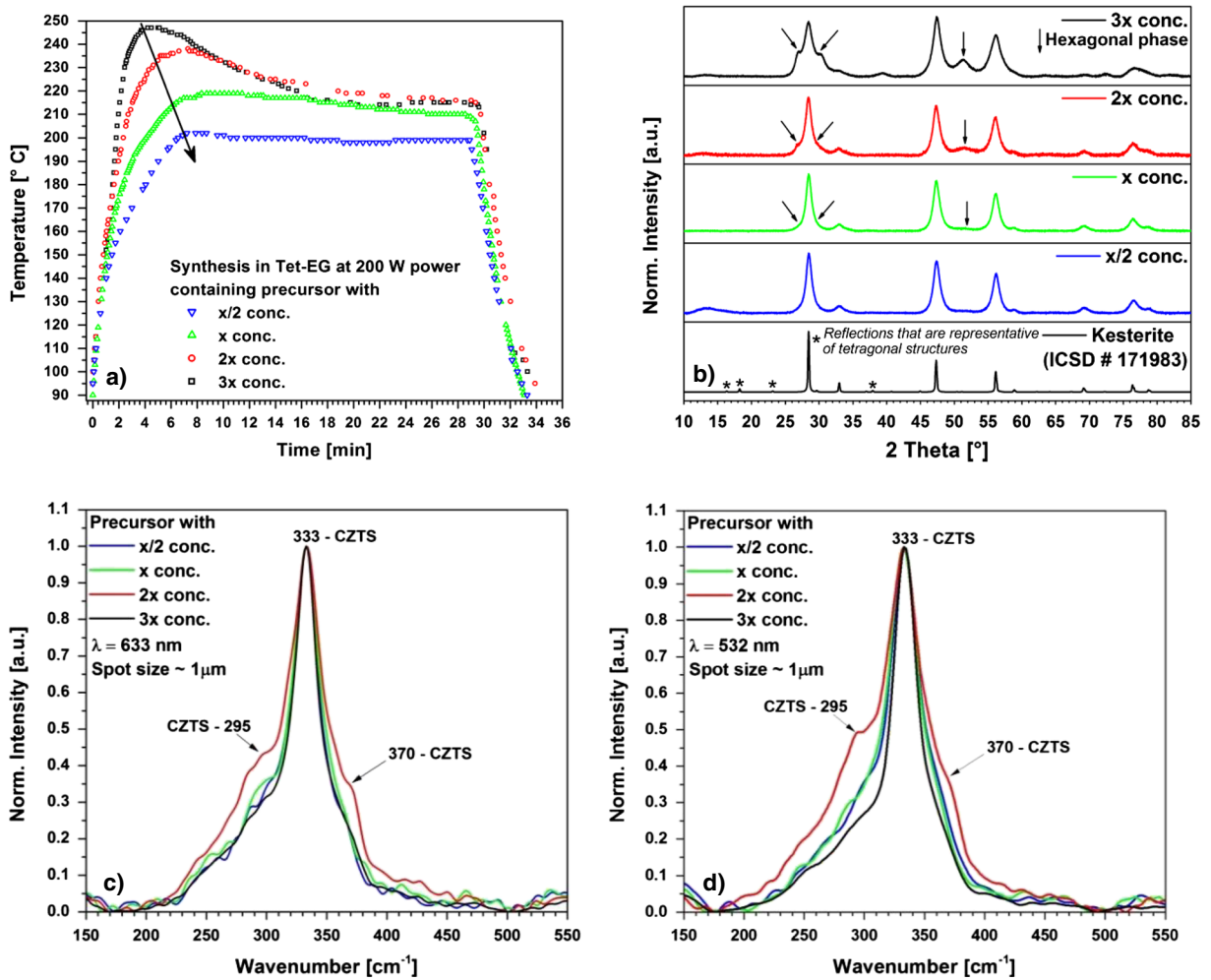


Fig. 4 **a** Temperature profiles obtained during the synthesis of CZTS nanoparticles in tet-EG under 200 W power and using different precursor concentrations. Phase analysis of as-obtained nanoparticles by **b** XRD confirming the presence of cubic CZTS,

hexagonal phase (impurity) along with **c, d** Raman spectra using *red* and *green* lasers, respectively, that confirm the presence of CZTS phase

Again, a direct comparison of the product synthesized at 200 W in tet-EG using *x/2* concentration (Fig. 4) is possible with EG at 100 W using *x* concentration (Fig. 1). It can be observed that the two products are very similar; however, the product obtained in tet-EG appears to have least amounts of hexagonal phase impurity. Therefore, by changing the type of solvent, temperature (power) or concentration of precursors, the amount of by-products formed in a microwave-assisted synthesis of CZTS can be controlled and the reaction can be driven towards the more selective formation of CZTS phase.

Discussion

Development of a relationship between process parameters and product purity

The phase characterization of the CZTS nanoparticles synthesized under microwave irradiation shows that two kinds of by-products form, i.e. Cu_{2-x}S and a hexagonal phase impurity. The presence of Cu_{2-x}S can be easily ascertained by Raman analysis (Figs. 1c, d, 3c, d and 4c, d) whereas the hexagonal phase is identified by the shoulder to the most intense XRD reflection at $\sim 28.45^\circ$ (Figs. 1b, 3b and 4b). Concerning Cu_{2-x}S , the results indicate that an increase of

temperature helps to minimize the amount of Cu_{2-x}S (Figs. 1, 3 and 4). Moreover, a minimum temperature of $\sim 200^\circ\text{C}$ is required to remarkably suppress its formation. We have demonstrated throughout the paper that the achievement of this temperature depends on a number of parameters such as the power irradiation, the solvent and the concentration of precursors. On the contrary, the formation of the hexagonal phase does not show a direct dependence on temperature. In fact, while Figs. 1 and 3 suggest that with increasing power, and hence temperature, the amount of hexagonal phase is also reduced, and the set of experiments in Fig. 4 suggest an opposite trend, i.e. the higher the temperature, the higher the amount of hexagonal phase impurity. To rationalize these results and to develop a relationship between process parameters and product purity, a specific energy factor (Eq. 1) can be calculated using the time-temperature profiles of reactions and the free energy of formation for CZTS ($\Delta G_{\text{f}}(\text{CZTS})$) estimated from the work of Baryshev and Thimsen (2015).

Specific energy factor

$$= \frac{M \text{ (kg)} \times C_p \text{ (J kg}^{-1} \text{ K}^{-1}) \times \Delta T \text{ (K)}}{\text{Free energy of formation of CZTS } (\Delta G_{\text{f}}) \text{ (J)}} \quad (1)$$

where M and C_p are the total mass and specific heat capacity of precursors and solvent and ΔT is the change in temperature of the reaction mixture. The detailed calculations are provided in supporting information. It must be noted that in contrast to conventional synthesis protocols (where a fixed time-temperature profile is given as an input parameter), in our experiments the heating ramp and temperature during the particle formation are an outcome of the supplied microwave power and how the reaction mixture interacts with it. The system is allowed to achieve any heating rate and temperature. Therefore, the specific energy factor is the ratio of the energy changes that take place during the course of reaction as observed by changes in temperature and the free energy of formation of CZTS ($\Delta G_{\text{f}}(\text{CZTS})$). Due to the fact that the formation of CZTS is an exothermic process, the free energy of formation is negative and, therefore, also the specific energy factor (F) is negative. The higher the absolute value of F , the higher the amount of energy per mole (solvent and precursors) during the course of the reaction with respect to the minimum amount of energy that is necessary to provide to the system to form the CZTS phase.

A comparison of specific energy factors (F) (Table 2) for different reactions and the phase analysis presented in Figs. 1, 3 and 4 shows that the product purity can be related to F . For this purpose, the occurrence of Cu_{2-x}S phase was evaluated from the Raman spectra as the ratio between the peak at 333 cm^{-1} that is due to CZTS and the peak at 472 cm^{-1} that is due to Cu_{2-x}S (Table 2). Similarly, the occurrence of the hexagonal phase was evaluated from the XRD pattern as the ratio between the reflection at $26.85^\circ (2\theta)$ and $28.45^\circ (2\theta)$ (Table 2).

In the first set of experiments (Fig. 1), the synthesis in EG produces the purest product (Table 2, line 1) as compared to tet-EG (Table 2, line 4). If we compare the values of F for these two experiments, we find $F = -124.64$ for the former and $F = -86.26$ for the latter. Similarly, as the power of microwaves (Fig. 3) is increased in the second set of experiments (while keeping all other variables constant), the purity of product increases from 100 W with $F = -86.26$ (line 4 in Table 2) to 200 W with $F = -139.16$ (line 6 in Table 2). Finally, in the last set of experiments, the concentration of precursors is varied (Fig. 4). When the $x/2$ concentration was used, no evidences of Cu_{2-x}S phase as well as of hexagonal phase were detected, leading to the most phase pure CZTS particles (line 7, Table 2). For this experiment, a value of $F = -242.45$ is calculated. If the latter result is compared with the results of the $3x$ concentration experiment where the highest amount of hexagonal phase is observed (line 9, Table 2), a value of $F = -51.64$ is found. Therefore, a correlation between the specific energy factor (F) and the phase purity can be established; i.e. the more negative the value of F , the higher the energy per mole and the highest the product purity. A value of F as high as -242 allows the synthesis of CZTS nanoparticles without any presence of detectable amounts of Cu_{2-x}S phase as well as hexagonal phase.

However, it is important to underline here that the correlation between F and the product purity must be considered only as a relative parameter to give hints about the quality of CZTS particles. In fact, the absolute amounts of by-products in different phases are hard to be estimated and the free energy of formation of CZTS is also not yet known with good reliability (Baryshev and Thimsen 2015). Nevertheless, we believe that the use of this parameter can provide a tool to design the rational synthesis of high-quality CZTS particles towards secondary-phase free products. Based on the results of this work, it is preferable to use a polar solvent

with a high boiling point (>200 °C) where a screening of the process parameters can be run more effectively.

Conclusion

In the current paper, the influence of process parameters on the phase purity of CZTS nanoparticles synthesized under microwave irradiation has been investigated in depth. In a first instance, it has been shown that the correct assessment of temperature during the microwave-assisted synthesis is of paramount importance and cannot be realized via the non-contact infrared sensor. A simple method using a standard glass non-mercury thermometer immersed in the reaction mixture has shown that the temperature during the reaction is much higher than that reported by the in-built non-contact infrared sensor. This correct assessment of temperature-time profile sets the basis for defining a specific energy factor (F) that can be correlated to the phase purity of CZTS particles.

Moreover, a tool box consisting of green solvents, power of microwaves and precursors concentration has been presented to control the temperature-time profile. Therefore, by varying these parameters, the phase purity of CZTS nanoparticles can be controlled systematically. According to the state of the art, EG is the most widely used solvent for the synthesis of CZTS under microwave conditions. However, due to its boiling point (197 °C), it offers limited possibilities to tune the process parameters at atmospheric pressure. Therefore, tet-EG, with a boiling point of 329 °C, was used in the current work to demonstrate how the phase purity of CZTS particles can be improved by tuning process parameters such as irradiation power and concentration of precursors.

In particular, two kinds of by-products have been observed throughout the work, i.e. Cu_{2-x}S and a hexagonal phase, based on EDX analysis in combination with the ICP-OES analysis of the mother liquor. It has been observed that an increased working temperature favours the reduction of Cu_{2-x}S (which is thermodynamically far less favourable product than CZTS) (Ahmad et al. 2013). In this regard, a temperature higher than 200 °C is required to suppress the formation of the Cu_{2-x}S phase. However, the amounts of hexagonal phase cannot be scaled with the temperature only. Therefore, a specific energy factor (F) has been introduced and its value correlated with the overall phase purity of the CZTS particles, i.e. the more negative the value of F , the higher the energy per mole and the product purity. A value of F as high as -242 allows the

synthesis of CZTS nanoparticles without any presence of detectable amounts of Cu_{2-x}S as well as hexagonal phase.

We believe that this paper not only offers a reliable protocol for the synthesis of CZTS nanoparticles but also sets the framework for predicting the phase purity of CZTS materials produced under microwave irradiation.

Acknowledgements This work was supported by the Deutsche Forschungsgemeinschaft through the Cluster of Excellence “Engineering of Advanced Material” initiative at the “Friedrich Alexander University of Erlangen-Nuremberg”. The authors also thank Dipl. – Ing. Andreas Güldenpfennig for the fruitful discussion and Dipl. Ing. Paula Hoppe for the assistance in ICP-OES analysis.

Conflict of interest The authors declare that they have no conflict of interest.

References

- Abramoff MD, Magalhães PJ, Ram SJ (2004) Image processing with Image J. *Biophotonics Int.* <http://dSPACE.library.uu.nl/handle/1874/204900>. Accessed 12 Apr 2016
- Ahmad R, Brandl M, Distaso M, et al (2015) A comprehensive study on the mechanism behind formation and depletion of $\text{Cu}_2\text{ZnSnS}_4$ (CZTS) phases. *CrystEngComm*. doi: 10.1039/C5CE00661A
- Ahmad R, Distaso M, Azimi H et al (2013) Facile synthesis and post-processing of eco-friendly, highly conductive copper zinc tin sulphide nanoparticles. *J Nanopart Res* 15:1–16. doi:10.1007/s11051-013-1886-9
- Azimi H, Hou Y, Brabec CJ (2014) Towards low-cost, environmentally friendly printed chalcopyrite and kesterite solar cells. *Energy Environ Sci* 7:1829–1849. doi:10.1039/C3EE43865A
- Baryshev SV, Thimsen E (2015) Enthalpy of formation for Cu-Zn-Sn-S (CZTS) calculated from surface binding energies experimentally measured by ion sputtering. *Chem Mater* 27: 2294–2298. doi:10.1021/cm504749d
- Bilecka I, Niederberger M (2010) Microwave chemistry for inorganic nanomaterials synthesis. *Nano* 2:1358–1374. doi:10.1039/B9NR00377K
- Brandl M, Ahmad R, Distaso M et al (2015) In-situ X-ray diffraction analysis of the recrystallization process in $\text{Cu}_2\text{ZnSnS}_4$ nanoparticles synthesised by hot-injection. *Thin Solid Films* 582:269–271. doi:10.1016/j.tsf.2014.10.077
- Carrete A, Shavel A, Fontané X et al (2013) Antimony-based ligand exchange to promote crystallization in spray-deposited $\text{Cu}_2\text{ZnSnS}_4$ solar cells. *J Am Chem Soc* 135: 15982–15985. doi:10.1021/ja4068639
- Chen S, Tao H, Shen Y et al (2014) Facile synthesis of single crystalline sub-micron $\text{Cu}_2\text{ZnSnS}_4$ (CZTS) powders using solvothermal treatment. *RSC Adv* 5:6682–6686. doi:10.1039/C4RA12815J
- Choi HW, Zhou T, Singh M, Jabbour GE (2015) Recent developments and directions in printed nanomaterials. *Nano* 7:3338–3355. doi:10.1039/C4NR03915G
- Cui H, Feng Y, Ren W et al (2009) Strategies of large scale synthesis of monodisperse nanoparticles. *Recent Pat Nanotechnol* 3:32–41

- Cushing BL, Kolesnichenko VL, O'Connor CJ (2004) Recent advances in the liquid-phase syntheses of inorganic nanoparticles. *Chem Rev* 104:3893–3946. doi:10.1021/cr030027b
- Delbos (2012) Kesterite thin films for photovoltaics: a review. *EPJ Photovolt* 3:13. doi:10.1051/epjpv/2012008
- Dimitrievska M, Fairbrother A, Fontané X, Jawhari T, Izquierdo-Roca V, Saucedo E, Pérez-Rodríguez A (2014) Multiwavelength excitation Raman scattering study of polycrystalline kesterite $\text{Cu}_2\text{ZnSnS}_4$ thin films. *Appl Phys Lett* 104(2):021901
- Distaso M, Mačković M, Spiecker E, Peukert W (2012a) Early stages of oriented attachment: formation of twin ZnO nanorods under microwave irradiation. *Chem Eur J* 18:13265–13268. doi:10.1002/chem.201201646
- Distaso M, Mačković M, Spiecker E, Peukert W (2014) Formation and dissolution of twin ZnO nanostructures promoted by water and control over their emitting properties. *Chem Eur J* 20:8199–8209. doi:10.1002/chem.201400100
- Distaso M, Segets D, Wernet R et al (2012b) Tuning the size and the optical properties of ZnO mesocrystals synthesized under solvothermal conditions. *Nano* 4:864–873. doi:10.1039/C1NR11226K
- Dudley GB, Richert R, Stigman AE (2015) On the existence of and mechanism for microwave-specific reaction rate enhancement. *Chem Sci* 6:2144–2152. doi:10.1039/C4SC03372H
- Fernandes PA, Salomé PMP, da Cunha AF (2011) Study of polycrystalline $\text{Cu}_2\text{ZnSnS}_4$ films by Raman scattering. *J Alloys Compd* 509(28):7600–7606
- Flynn B, Wang W, Chang C, Herman GS (2012) Microwave assisted synthesis of $\text{Cu}_2\text{ZnSnS}_4$ colloidal nanoparticle inks. *Phys Status Solidi A* 209:2186–2194. doi:10.1002/pssa.201127734
- Gerbec JA, Magana D, Washington A, Strouse GF (2005) Microwave-enhanced reaction rates for nanoparticle synthesis. *J Am Chem Soc* 127:15791–15800. doi:10.1021/ja052463g
- Ghorpade U, Suryawanshi M, Shin SW et al (2014) Towards environmentally benign approaches for the synthesis of CZTSSe nanocrystals by a hot injection method: a status review. *Chem Commun* 50:11258–11273. doi:10.1039/C4CC03176H
- He Y, Lu H-T, Sai L-M et al (2006) Microwave-assisted growth and characterization of water-dispersed CdTe/CdS core-shell nanocrystals with high photoluminescence. *J Phys Chem B* 110:13370–13374. doi:10.1021/jp057498h
- Hermes W, Waldmann D, Agari M et al (2015) Emerging thin-film photovoltaic technologies. *Chem Ing Tech* 87:376–389. doi:10.1002/cite.201400101
- Just J, Lützenkirchen-Hecht D, Frahm R, Schorr S, Unold T (2011) Determination of secondary phases in kesterite $\text{Cu}_2\text{ZnSnS}_4$ thin films by x-ray absorption near edge structure analysis. *Appl Phys Lett* 99(26):262105
- Kim J, Hiroi H, Todorov TK et al (2014) High efficiency $\text{Cu}_2\text{ZnSn}(\text{S}, \text{Se})_4$ solar cells by applying a double $\text{In}_2\text{S}_3/\text{CdS}$ emitter. *Adv Mater* 26:7427–7431. doi:10.1002/adma.201402373
- Knutson TR, Hanson PJ, Aydi ES, Penn RL (2014) Synthesis of $\text{Cu}_2\text{ZnSnS}_4$ thin films directly onto conductive substrates via selective thermolysis using microwave energy. *Chem Commun* 50:5902–5904. doi:10.1039/C3CC49207A
- Lin Y-H, Das S, Yang C-Y et al (2015) Phase-controlled synthesis of $\text{Cu}_2\text{ZnSnS}_4$ powders via the microwave-assisted solvothermal route. *J Alloys Compd* 632:354–360. doi:10.1016/j.jallcom.2015.01.254
- Martini T, Chubilleau C, Poncelet O et al (2016) Spray and inkjet fabrication of $\text{Cu}_2\text{ZnSnS}_4$ thin films using nanoparticles derived from a continuous-flow microwave-assisted synthesis. *Sol Energy Mater Sol Cells* 144:657–663. doi:10.1016/j.solmat.2015.09.046
- Morschhäuser R, Krull M, Kayser C et al (2012) Microwave-assisted continuous flow synthesis on industrial scale 1:281–290
- Pein A, Baghbanzadeh M, Rath T et al (2011) Investigation of the formation of CuInS_2 nanoparticles by the oleylamine route: comparison of microwave-assisted and conventional syntheses. *Inorg Chem* 50:193–200. doi:10.1021/ic101651p
- Saravana Kumar R, Hong C-H, Kim M-D (2014) Doughnut-shaped hierarchical $\text{Cu}_2\text{ZnSnS}_4$ microparticles synthesized by cyclic microwave irradiation. *Adv Powder Technol* 25:1554–1559. doi:10.1016/j.apt.2014.05.005
- Shin SW, Han JH, Park C-Y et al (2012) Quaternary $\text{Cu}_2\text{ZnSnS}_4$ nanocrystals: facile and low cost synthesis by microwave-assisted solution method. *J Alloys Compd* 516:96–101. doi:10.1016/j.jallcom.2011.11.143
- Siebert S (2013) Why are kesterite solar cells not 20% efficient? *Thin Solid Films* 535:1–4. doi:10.1016/j.tsf.2012.12.089
- Sun C, Gardner JS, Long G et al (2010) Controlled stoichiometry for quaternary $\text{CuIn}_x\text{Ga}_{1-x}\text{S}_2$ chalcopyrite nanoparticles from single-source precursors via microwave irradiation. *Chem Mater* 22:2699–2701. doi:10.1021/cm100456t
- Kharisova OV, Kharisov BI, Méndez UO (2011) Microwave-assisted synthesis of coordination and organometallic compounds. In: Grundas S (ed) *Advances in induction and microwave heating of mineral and organic materials*. InTech. doi:10.5772/13149
- Vaccarello D, Liu L, Zhou J, Sham T-K, Ding Z (2015) Photoelectrochemical and physical insight into $\text{Cu}_2\text{ZnSnS}_4$ nanocrystals using synchrotron radiation. *J Phys Chem C* 119(21):11922–11928
- van Embden J, Chesman ASR, Jasieniak JJ (2015) The heat-up synthesis of colloidal nanocrystals. *Chem Mater* 27:2246–2285. doi:10.1021/cm5028964
- Wang K-C, Chen P, Tseng C-M (2013) Facile one-pot synthesis of $\text{Cu}_2\text{ZnSnS}_4$ quaternary nanoparticles using a microwave-assisted method. *CrystEngComm* 15:9863–9868. doi:10.1039/C3CE41691G
- Wu C-C, Shiau C-Y, Ayele DW et al (2010) Rapid microwave-enhanced solvothermal process for synthesis of CuInSe_2 particles and its morphologic manipulation. *Chem Mater* 22:4185–4190. doi:10.1021/cm1006263
- Yan X, Hu X, Komarneni S (2015) Solvothermal synthesis of CZTS nanoparticles in ethanol: preparation and characterization. *J Korean Phys Soc* 66:1511–1515. doi:10.3938/jkps.66.1511
- Zhao Y, Tao W, Chen X et al (2015a) Synthesis and characterization of $\text{Cu}_2\text{ZnSnS}_4$ nanocrystals prepared by microwave irradiation method. *J Mater Sci Mater Electron* 26:5645–5652. doi:10.1007/s10854-015-3114-0
- Zhao Y, Tao W, Liu J, Wei A (2015b) Rapid synthesis of $\text{Cu}_2\text{ZnSnS}_4$ nanocrystalline thin films directly on transparent conductive glass substrates by microwave irradiation. *Mater Lett* 148:63–66. doi:10.1016/j.matlet.2015.02.068
- Zhou H, Hsu W-C, Duan H-S et al (2013) CZTS nanocrystals: a promising approach for next generation thin film photovoltaics. *Energy Environ Sci* 6:2822–2838. doi:10.1039/C3EE41627E